



ISSN: 0975-833X

Available online at <http://www.journalcra.com>

INTERNATIONAL JOURNAL
OF CURRENT RESEARCH

International Journal of Current Research
Vol. 13, Issue, 09, pp.18856-18861, September, 2021

DOI: <https://doi.org/10.24941/ijcr.42096.09.2021>

RESEARCH ARTICLE

SYNTHESIS OF NANOPARTICULATE SYSTEM FOR CONTROLLED RELEASE OF DRUGS, WITH THERMAL, STRUCTURAL, MORPHOLOGICAL AND MAGNETIC PROPERTIES

Artur E. A. de Castro^{1,*}, Alejandra H. M. González², Daniel Cornejo³, Rafael R. G. Paranhos⁴, Ricardo L. Tranquilin⁵, Roberto da Silva Gusmão¹, Regina M. S. Pereira¹ and Márcio L. dos Santos¹

¹Programa de Biotecnologia e Inovação em Saúde, Universidade Anhanguera de São Paulo, São Paulo, SP, Brazil

²Departamento de Odontologia Restaurativa, Faculdade de Odontologia, Universidade do Norte do Paraná, Londrina, PR, Brazil

³Departamento de Física dos Materiais e Mecânica, Instituto de Física, Universidade de São Paulo - USP, São Paulo, SP, Brazil

⁴CDMF-LIEC, UFSCar, P.O. Box 676, 13565-905 São Carlos, SP, Brazil

ARTICLE INFO

Article History:

Received 29th June, 2021

Received in revised form

24th July, 2021

Accepted 19th August, 2021

Published online 30th September, 2021

Key Words:

Magnetic Nanoparticle,
Magnetite,
Doxorubicin,
Antitumor.

*Corresponding author:

Artur E. A. de Castro

ABSTRACT

Iron oxide magnetic nanoparticles (IONPs) have been used in biomedical applications as carriers for drug delivery, magnetic resonance imaging, magnetic hyperthermia and thermoablation, bioseparation and biosensor applications. The aim of this study was to synthesize magnetite nanoparticles coated with silica and functionalized with Octadecyl Trimethoxy silane for future aggregation of anti-tumor, anti-inflammatory and other drugs in the intention of guided administration by external magnetic systems such as: nuclear magnetic resonance, electromagnets and Neodymium magnets. Magnetic IONPs were synthesized by oxidation method adapted from literature, coated with silica, functionalized with Octadecyl Trimethoxy silane and saturated with Doxorubicin solution for future biomedical applications. The coated and functionalized magnetic IONPs were characterized by X-ray diffraction (XRD), Fourier transform infrared spectroscopy (FTIR), thermogravimetric analysis (TG), particle size and morphology by scanning electron microscopy (SEM) and magnetic properties analysis (ZFC curves). The analyses revealed that the functionalization of the coating and the incorporation of antitumor did not interfere with the magnetic properties of magnetite. The nanoparticles obtained are within the expected parameters for application as a guided drug delivery system.

Copyright © 2021. Artur E. A. de Castro et al. This is an open access article distributed under the Creative Commons Attribution License, which permits unrestricted use, distribution, and reproduction in any medium, provided the original work is properly cited.

Citation: Artur E. A. de Castro, Alejandra H. M. González, Daniel Cornejo, Rafael R. G. Paranhos et al. "Synthesis of nanoparticulate system for controlled release of drugs, with thermal, structural, morphological and magnetic properties.", 2021. International Journal of Current Research, 13, (09), 18856-18861.

INTRODUCTION

Human cancer has several causes, such as: environmental, dietary, genetic disposition, among others (BIZARI et al., 2006). Cancer treatments are aggressive and the development of resistance to chemotherapy and radiotherapy have been the main concern in treatment (ARRUEBO et al., 2011). Therefore, there is an urgent need to develop diagnostics and treatments to improve the prognosis of these patients. In the last thirty years, the search for new treatments has caused an advance in the development of nano formulations.

Nanoparticles can be classified as organic (lipids, liposomes, polymers, polymeric micelles, peptides and nucleic acids) (CLAUSON et al., 2018; ONG et al., 2018) and inorganic (carbon nanoparticles, metal and metal oxide nanoparticles) (GAO et al., 2016; LEGGE et al., 2018; XIE et al., ZHANG et al., 2016). The special interest of the present study was to use magnetic iron oxide nanoparticles (IONPs) at first as drug vehicles for future testing in the treatment of bone and breast cancer. Iron oxides are compounds found in nature and can also be synthesised (GUPTA and GUPTA, 2005). In the last decade, magnetic IONPs have been prominent in biomedicine, being used as drug vehicles in guided therapy, magnetic

resonance imaging (MRI), magnetic hyperthermia and thermoablation, bioseparation, and biosensing (FERRARI, 2010; WU *et al.*, 2015; ZHANG *et al.*, 2020). Magnetic IONPs are very versatile, and can be used in different core sizes, surface functionalization, and drug-loading capabilities (FANG *et al.*, 2020; GUARDIA *et al.*, 2010; WU *et al.*, 2015). The use of mesoporous silica as nanoparticle coatings is a strategy that has been used to obtain "smarter" and more effective nanoparticles, comprising synthesis techniques and properties, biocompatibility techniques, functionalization, as well as coatings that ensure drug delivery to the target of choice (NIK *et al.*, 2020; TENG *et al.*, 2020). In this work, IONPs nanoparticles were synthesized, coated, functionalized and saturated with Doxorubicin (Dx), one of the drugs used in the treatment of bone tumors, according to adaptations of the techniques of Stöber *et al.* and Qu *et al.* (STÖBER *et al.*, 1968; and QU *et al.*, 1999).

MATERIALS AND METHODS

Synthesis of magnetite: The synthesis was carried out by means of a chemical oxy reduction route with ferric chloride, sodium sulfite and ammonium hydroxide, adapted (STÖBER *et al.*, 1968; and QU *et al.*, 1999). The synthesized product was stored in a hermetically sealed container.

Coating of magnetite with silica (MagSi): The magnetite was coated with silica. Tetraethyl Orthosilicate (TEOS) was added. The resulting particle was dried and kept in a hermetically sealed container.

Functionalisation using n-octadecyl trimethoxy silane (MagSiF): Tetraethyl Orthosilicate was mixed with n-Octadecyl Trimethoxy silane and incorporated into the coated magnetic nanoparticle and the obtained product was kept in a hermetically sealed container.

Loading of Doxorubicin on Functionalized Magnetite (MagSiFDx): The drug (Doxorubicin) adsorption step was based on Liberman *et al.*, with modifications (LIBERMAN *et al.*, 2014). The nanoparticles obtained in the three synthesis steps, MagSi, MagSiF and MagSiFDx were characterized by X-ray diffraction, infrared (IR) spectroscopy, magnetization, particle size measurements, Transmission Electron Microscopy (TEM), Dynamic Light Scattering (DLS) and magnetic properties (ZFC curves).

RESULTS AND DISCUSSION

The reason for the functionalization is to promote the interaction with the antitumor in such a way to keep it aggregated until it reaches the site of action in vivo, where it would initiate its release. The nano particulate nucleus, constituted of magnetite (Fe₃O₄), would be subject to the maintenance of a magnet placed externally on the site of application of the proposed formulation, preventing its distancing from the site of action.

X-ray diffraction: The evidence of large peaks in this sample is given by the nanometric size of the crystals, which results in a reduction in the number of crystalline planes. Fig. 1 shows the X-ray diffractograms of Magnetite (Mag) and the

corresponding standards, a series of characteristic peaks (220), (311), (400), (422), (440) and (511), which are in agreement with the cubic phase of Fe₃O₄ (magnetite, JCPDS No. 85-1436). Doxorubicin incorporation did not cause changes in the XRD pattern, as none of the Dx-related peaks were observed in the MagSiFDx sample. This indicates that Dx, when incorporated into magnetite, is not covering the surface of the coated magnetic nanoparticles but, rather, probably in the porosity created by Octadecyl functionalisation. However, when analysing the 2θ range from 10 to 25°, a degree of amorphism was observed in all diffractograms, which is possibly related to the incorporation of organic binders into the magnetite. According to the diffractograms, the oxy reduction method was suitable for the synthesis of magnetite.

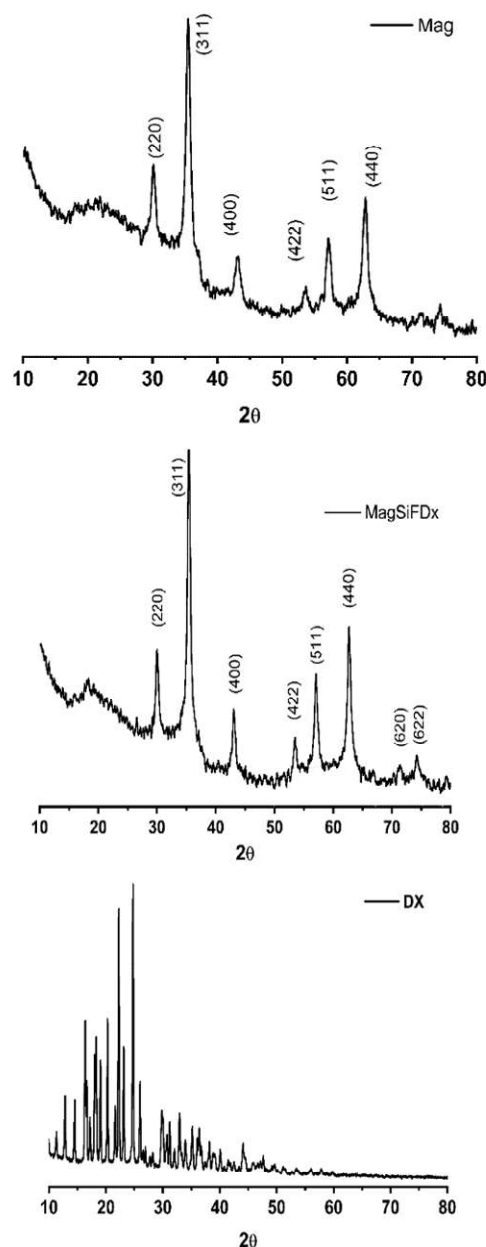


Figure 1. X-ray diffractograms: Magnetite (Mag); silica coated Magnetite, functionalised with Octadecyl trimethoxy silane and doped with Doxorubicin (MagSiFDx) and Doxorubicin (Dx)

Fourier transform mid-infrared absorption spectroscopy – FTIR: The FTIR spectra of Mag, MagSi, MagSiF, MagSiFDx and Dx are shown in fig. 2. The magnetized structure of Fe^{III} (Fe^{II}Fe^{III}) O₄ can show four active models in the R.I. spectrum for each structure but, in several situations, two

modes are weakly expressed and, evidently, at low wavelengths (FARJADIAN *et al.*, 2016; GUILLOT *et al.*, 1983). The infrared spectrum of magnetite showed two large absorption bands at 620 and 468 cm^{-1} , vibrations characteristic of the Fe-O stretching mode of magnetite in good agreement with the data obtained by other authors (ROCA *et al.*, 2009; SOUZA *et al.*, 2008). The broad band 3443 cm^{-1} relative to the stretching of the -OH groups and the band 1627 cm^{-1} attributed to the deformation of the H-O-H bond suggest the presence of water adsorbed on the particle surface. The MagSi spectrum showed a broad band at 1093 cm^{-1} characteristic of the asymmetric stretching of the Si-O-Si bonds (BRUNI *et al.*, 1999). The band observed at 790 cm^{-1} is associated with the symmetric stretching of the Si-O bond and the band at 462 cm^{-1} is related to the Si-O-Si tensioning vibration mode. The presence of free Si-OH silanols on the particle surface is confirmed by the band at 942 cm^{-1} and two main absorption bands at 647 and 550 cm^{-1} , vibrations characteristic of the Fe-O magnetite stretching mode.

The 3450 cm^{-1} wide bands related to the stretching of the -OH groups and the 1623 cm^{-1} band attributed to the deformation of the H-O-H bond suggest the presence of water adsorbed on the particle surface (CORINNE and CORINNE, 1996). In the FTIR spectrum of MagSiF, a broad band was observed at 3470 cm^{-1} relative to the elongation of the -OH groups or the vibration of the elongation of the -OH groups of silanol (Si-OH), and the band at 1620 cm^{-1} assigned to the deformation of the HOH bond suggests the presence of water adsorbed on the particle surface (CORINNE and CORINNE, 1996). The stretching vibration of the Si-O-Si bond gives rise to the broad and intense absorption bands at 1210 and 1050 cm^{-1} (SAMBANDAM and RAMANI, 2007). The absorption at 710 cm^{-1} and 480 cm^{-1} are attributed to the asymmetric vibration of the siloxane network and the flexural vibration of the Si-O bond (SAMBANDAM and RAMANI, 2007). The absorption band at 640 cm^{-1} corresponds to the characteristic vibration of the Fe-O stretching mode of magnetite (ROCA *et al.*, 2009). In the FTIR spectra of MagSiFDx and Doxorubicin (Dx), a broad band at 3445 cm^{-1} can be observed in relation to the stretching of the OH- group or H-OH deformation for drug encapsulation. The band at 462 cm^{-1} is related to the vibration mode of the Si-O-Si group. The spectrum of Doxorubicin encapsulated by functionalised magnetic nanoparticles, indicated that there was a propensity for magnetic nanoparticles to interact with drugs through co-precipitation method (QU *et al.*, 1999). Typical bands of pure drug and nanoparticles as well as C = O and C = C functional groups can be observed at 1630 and 1440 cm^{-1} , indicating the effective incorporation of the drug into the polymer matrix. Bands before 1000 cm^{-1} are fingerprint regions of the drug and functionalised magnetite. Therefore, the drug-magnetite interaction can be realized using chemical bonds between functional molecules such as OH, CH, CN, CO, C = O and / or C = C and physical association between magnetite and / or drug molecules. Doxorubicin showed distinct bands 587, 790, 870, 995, 1067, 1180, 1427, 1520, 1630, 1740, 2912, 3055, 3339 and 3523 cm^{-1} may correspond to alkane groups CH, Aromatic CH, carboxylic acids, elongation of C-alkene = C, NH₃ structure, charged amines C = NH⁺ and H-OH.

Thermal analysis: Fig. 3 shows the thermogravimetric curves of the Mag, Dx and MagSiFDx samples and, in the Mag sample, an initial mass loss at 61.78 $^{\circ}\text{C}$ can be observed.

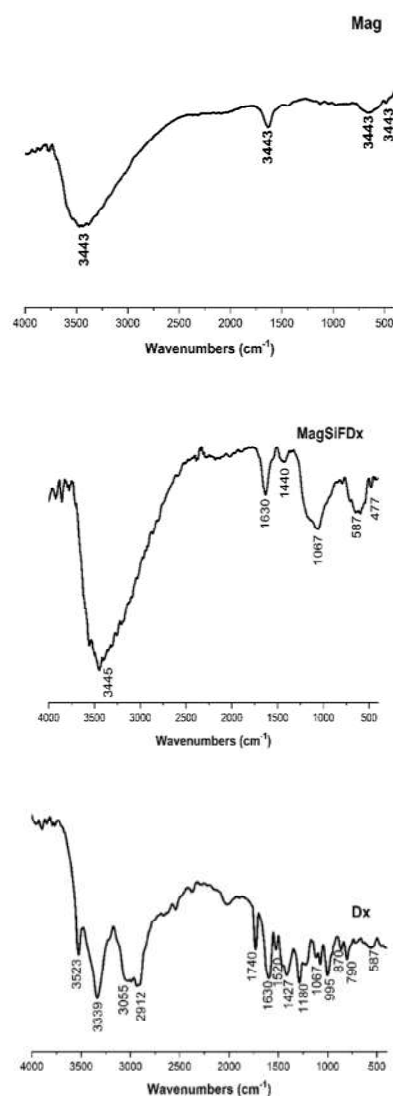


Figure 2. FTIR spectra: Magnetite (Mag), Doxorubicin (Dx) and silica-coated Magnetite functionalized with Octadecyl Trimethoxy Silane and loaded with Doxorubicin (MagSiFDx)

It is also possible to observe an initial mass loss at 146.27 $^{\circ}\text{C}$. This reduction of about 5.1% of the total mass can be attributed to the loss of water molecules adsorbed on the magnetite surface. From 146.27 $^{\circ}\text{C}$ to 355.92 $^{\circ}\text{C}$ a mass loss of approximately 1.3% is observed which may be associated with the combustion of residual organic material (HONG *et al.*, 2008, ISHIKAWA *et al.*, 1998, JITIANU *et al.*, 2006). MagSiFDx shows the TG curve obtained for the functionalised magnetite coated silica saturated with Doxorubicin. Two stages of mass loss can be observed, with a total reduction of 40% in mass. The first reduction occurs at 34.26 $^{\circ}\text{C}$ and can be attributed to the loss of adsorbed water molecules and dehydration. The second mass reduction at 262.77 $^{\circ}\text{C}$ can be attributed to the combustion of residual organic matter and incorporation of the drug by magnetic nanoparticles, observing a 0.8% mass reduction. The third step from 400 $^{\circ}\text{C}$ onwards may be related to the restructuring of the structure of the functionalised magnetite and the incorporated drug. Dx shows the TG curve obtained for Doxorubicin. Three stages of mass loss can be observed, with a total mass reduction of 50%. The first loss at 182.59 $^{\circ}\text{C}$, of approximately 30%, refers to dehydration, while, the second refers to combustion of organic matter at 232.61 $^{\circ}\text{C}$ and, in the third step, to decomposition at 350.14 $^{\circ}\text{C}$.

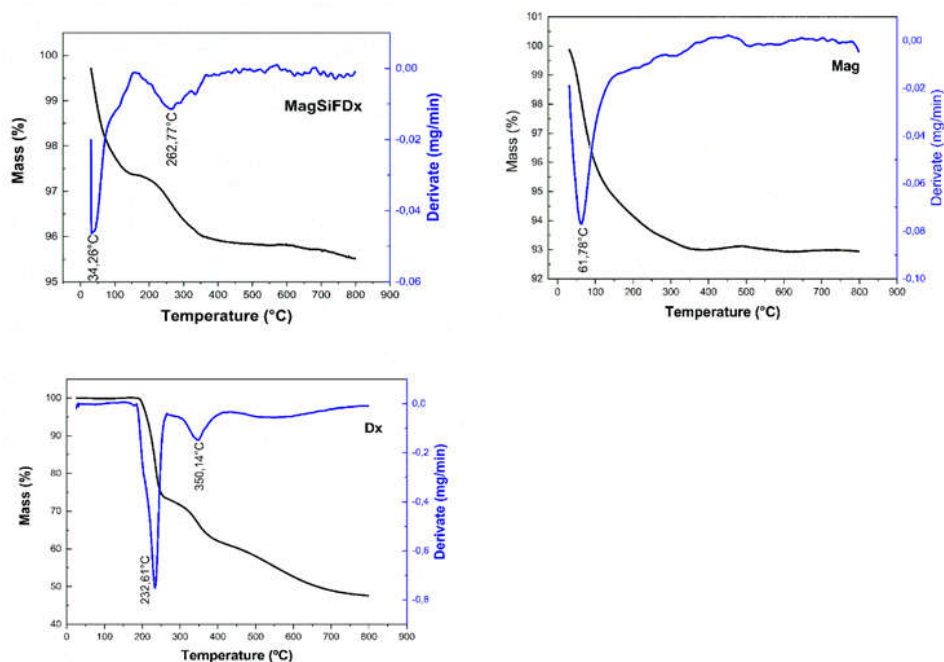


Figure 3. Magnetite (Mag); silica-coated magnetite, functionalised with Octadecyl trimethoxy silane, loaded with Doxorubicin (MagSiFDx); and Doxorubicin (Dx)

Table 1. Mean diameters and polydispersity results of Mag and MagSiFDx particles. Average of five tests

	Effective diameter average (nm) (Average of 5 tests)	Diameter (Standard Deviation)	Polydispersity (Average of 5 tests)	Polydispersity (Standard Deviation)
Mag	131,33	3,71	0,236	0,023
MagSiFDx	282,73	2,63	0,236	0,020

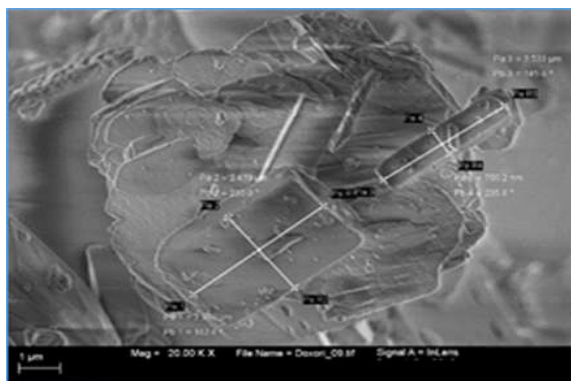


Figure 4. SEM micrographs: Magnetite (Mag), silica-coated magnetite, functionalized with octadecyl trimethoxy silane and saturated with Doxorubicin (MagSiFDx) and Doxorubicin (Dx)

Particle size: There was a concern to obtain particles smaller than 300 nm because this is the recommended diameter to cross the cell membrane (ARRUEBO *et al.*, 2007)31. Thus, the average effective diameter found in the Magnetite analysis (Table 1) was 131.33nm, with a polydispersity of 0.236, which represents a homogeneous size distribution (ARRUEBO *et al.*, 2007)31. Table 1 shows that particles smaller than 300 nm were obtained, fulfilling the cell permeability condition. At this stage, polydispersity was maintained at values that are often obtained by keeping the particle size homogeneous and close to the diameters between the particles formed by the formulation.

Scanning Electron Microscopy – SEM: The Magnetite (Mag) sample particles are shown in Fig. 4 (Mag), as expected, particle aggregation was observed since the specific surface area (surface to volume ratio) resulted in a high surface energy

and the particles are almost spherical, with an average size of 20nm (SILVA *et al.*, 2013). Fig. 4 (Dx) also illustrates the original Doxorubicin crystals (raw material) before dissolution and incorporation into the coated and functionalised magnetic particle. Fig. 4 (MagSiFDx) presents the image of silica-coated magnetite samples functionalised with Octadecyl trimethoxy silane and loaded with Doxorubicin, which did not substantially alter the morphology and size of the magnetite particle.

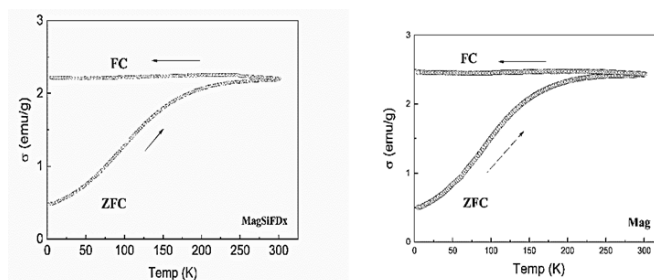


Figure 5. ZFC-FC curves: Magnetite (Mag); Magnetite coated with silica, functionalised with Octadecyl trimethoxy silane and loaded with Doxorubicin (MagSiFDx).

Analysis of the magnetic properties: Comparing the curves between Mag and MagSiFDx, there is a similarity in the magnetic behaviour of the two samples in fig. 5. The relative magnetization (magnetic moment per unit mass, in emu/g) increases with temperature in the ZFC curve, and after 250K this increase is slow, showing that the curve is approaching the maximum value. However, at 300K (maximum temperature of the experiment) the maximum value has not yet been reached.

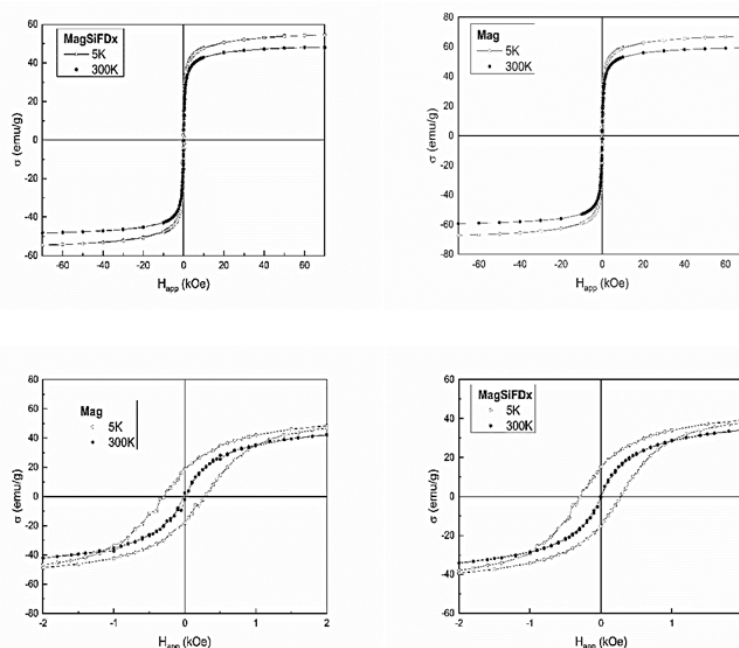


Figure 6. Magnetic hysteresis: Magnetite (Mag); Magnetite coated with silica, functionalised with Octadecyl trimethoxy silane and loaded with Doxorubicin (MagSiFDx)

The FC curve shows little variation with temperature. The maximum of the ZFC curve is expected to be at higher temperatures, but close to 300K. On the other hand, the near overlap of the ZFC and FC curves for values near 300 K shows that the nanoparticles are (at room temperature) in a magnetic reversibility regime (superparamagnetic regime). The separation of the ZFC and FC curves at low temperatures indicates that the magnetic nanoparticles present in the samples are in weak interaction, which is compatible with the fact that they are particles coated with non-magnetic material, which isolates them from each other. It is possible to observe the similar behaviour of both samples in Fig. 5. The second type of characterization performed consists in measuring hysteresis cycles at low temperature (5K) and at room temperature (300K). The results are shown in Fig. 6. The upper part of Mag shows the complete cycles (measured up to a maximum field of ± 70 kOe), while the lower part of MagSiFDx shows the behaviour of the same cycles, at low fields (in the range of ± 2 kOe). The cycles for the 5K temperature show hysteresis (area enclosed by the curves) with coercivities close to 0.3 kOe for both samples. This is compatible with the behaviours observed in other magnetite nanoparticle systems. At 300K, on the other hand, the coercivity is clearly zero (no area in the hysteresis loop), which shows that, in fact, the samples are superparamagnetic at room temperature. The saturation magnetization (maximum observed value of magnetization for 70 kOe) is approximately 60 emu/g for Magnetite (Mag) and 47 emu/g of the functionalized sample (MagSiFDx), both values corresponding to room temperature measurements.

CONCLUSION

The synthesis of Magnetite and other compositions was successfully carried out, considering that magnetic IONP were characterized by X-ray diffraction (XRD), Fourier transform infrared spectroscopy (FTIR), thermogravimetric analysis (TG), particle size and morphology by scanning electron microscopy (SEM) and magnetic properties analysis (ZFC curves) and the results revealed that the functionalization of the coating and incorporation of antitumor did not interfere in

the magnetic properties of Magnetite, showing that the particle obtained is perfectly within the parameters predicted for application as a drug delivery system, demonstrating structural and morphological properties similar to those obtained by other synthesis methodologies and, in particular, to the magnetic analyses that point to a possible application of systems such as drug delivery that act in the treatment of cancer tumours. However, further studies are needed to confirm the possible application.

ACKNOWLEDGMENTS

This work was supported by the Brazilian Science Agency - CAPES (Coordenação de Aperfeiçoamento de Pessoal de Nível Superior). Special thanks to the Department of Materials Physics and Mechanics, Institute of Physics, University of São Paulo - USP for performing the magnetic tests of nanoparticles and to CDMF-LIEC, UFSCar, PO Box 676, 13565-905 São Carlos, SP, Brazil, for further SEM tests.

REFERENCES

- Arruebo, M., Fernández-Pacheco, R., Ibarra, M.R., Santamaría, J. 2007. Magnetic nanoparticles for drug delivery The potential of magnetic NPs stems from the intrinsic properties of their magnetic cores combined with their drug loading capability and the biochemical properties that can be bestowed on them by means of a suitab, 2 pp. 22–32. <https://pdfs.semanticscholar.org/1844/8eb43dc235f82cb591983bc8df5ed799984c.pdf>.
- Arruebo, M., Vilaboa, N., Sáez-Gutierrez, B., Lambea, J., Tres, A., Valladares, M., González-Fernández, Á. 2011 Assessment of the evolution of cancer treatment therapies, *Cancers Basel*. 3 pp. 3279–3330. doi: 10.3390/cancers3033279.
- Bizari, L., Silva, A.E., Tajara, E.H. 2006 Gene amplification in carcinogenesis, *Genet. Mol. Biol.* 29 pp. 1–7. doi: 10.1590/S1415-47572006000100001.
- Bruni, S., Cariati, F., Casu, M., Lai, A., Musinu, A., Piccaluga, G., Solinas, S. 1999 IR and NMR study of nanoparticle-

- support interactions in a Fe₂O₃-SiO₂ nanocomposite prepared by a sol-gel method, *Nanostructured Mater.* 11 pp. 573–586. doi: 10.1016/S0965-97739900335-9.
- Clauson, R.M., Chen, M., Scheetz, L.M., Berg, B., Chertok, B. 2018 Size-Controlled Iron Oxide Nanoplatforns with Lipidoid-Stabilized Shells for Efficient Magnetic Resonance Imaging-Trackable Lymph Node Targeting and High-Capacity Biomolecule Display, *ACS Appl. Mater. Interfaces.* 10 pp. 20281–20295. doi: 10.1021/acsami.8b02830.
- Corinne ChanCac, E.T., Corinne ChanCac, J.P.J. 1996 Magnetic iron oxide-silica nanocomposites. *Synthesis and characterization*, 6 pp. 1905–1911.
- Fang, W., Zhu, W., Chen, H., Zhang, H., Hong, S., Wei, W., Zhao, T. 2020 MRI Enhancement and Tumor Targeted Drug Delivery Using Zn²⁺-Doped Fe₃O₄ Core/Mesoporous Silica Shell Nanocomposites, *ACS Appl. Bio Mater.* 3 pp. 1690–1697. doi: 10.1021/acsabm.9b01244.
- Farjadian, F., Ghasemi, S., Mohammadi-Samani, S. 2016 Hydroxyl-modified magnetite nanoparticles as novel carrier for delivery of methotrexate, *Int. J. Pharm.* 504 pp. 110–116. doi: 10.1016/j.ijpharm.2016.03.022.
- Ferrari, M. 2010 *Frontiers in cancer nanomedicine: Directing mass transport through biological barriers*, *Trends Biotechnol.* 28 pp. 181–188. doi: 10.1016/j.tibtech.2009.12.007.
- Gao, H. 2016 Progress and perspectives on targeting nanoparticles for brain drug delivery, *Acta Pharm. Sin. B.* 6 pp. 268–286. doi: 10.1016/j.apsb.2016.05.013.
- Guardia, P., Pérez, N., Labarta, A., Batlle, X. 2010 Controlled synthesis of iron oxide nanoparticles over a wide size range, *Langmuir.* 26 pp. 5843–5847. doi: 10.1021/la903767e.
- Guillot, M., Marchand, A., Nekvasil, Y., Tchéou, F. 1983 Anisotropic magnetic properties of samarium iron garnet in high magnetic field, *J. Magn. Magn. Mater.* 31–34 pp. 777–778. doi: 10.1016/0304-88538390680-7.
- Gupta, A.K., Gupta, M. 2005 Synthesis and surface engineering of iron oxide nanoparticles for biomedical applications, *Biomaterials.* 26 pp. 3995–4021. doi: 10.1016/j.biomaterials.2004.10.012.
- Hong, C.K., Hwang, I., Kim, N., Park, D.H., Hwang, B.S., Nah, C. 2008 Mechanical properties of silanized jute-polypropylene composites, *J. Ind. Eng. Chem.* 14 pp. 71–76. doi: 10.1016/j.jiec.2007.07.002.
- Ishikawa, T., Kondo, K., Yasukawa, A., Kandori, K. 1998 Formation of magnetite in the presence of ferric oxyhydroxides, *Corros. Sci.* 40 pp. 1239–1251. doi: 10.1016/S0010-938X9800045-6.
- Jitianu, A., Raileanu, M., Crisan, M., Predoi, D., Jitianu, M., Stanciu, L., Zaharescu, M. 2006 Fe₃O₄-SiO₂ nanocomposites obtained via alkoxide and colloidal route, *J. Sol-Gel Sci. Technol.* 40 pp. 317–323. doi: 10.1007/s10971-006-9321-7.
- Legge, E.J., Ahmad, M., Smith, C.T.G., Brennan, B., Mills, C.A., Stolojan, V., Pollard, A.J., Silva, S.R.P. 2018 Physicochemical characterisation of reduced graphene oxide for conductive thin films, *RSC Adv.* 8 pp. 37540–37549. doi: 10.1039/c8ra08849g.
- Liberman, A., Mendez, N., Trogler, W.C., Kummel, A.C. 2014 Synthesis and surface functionalization of silica nanoparticles for nanomedicine, *Surf. Sci. Rep.* 69 pp. 132–158. doi: 10.1016/j.surfrep.2014.07.001.
- Nik, A.B., Zare, H., Razavi, S., Mohammadi, H., Ahmadi, P.T., Yazdani, N., Bayandori, M., Rabiee, N., Mobarakeh, J.I. 2020 Smart drug delivery: Capping strategies for mesoporous silica nanoparticles, *Microporous Mesoporous Mater.* 299 pp. 110115. doi: 10.1016/j.micromeso.2020.110115.
- Ong, Y.S., Yazan, L.S., Ng, W.K., Abdullah, R., Mustapha, N.M., Sapuan, S., Foo, J.B., Tor, Y.S., How, C.W., Rahman, N.A., Ansar, F.H.Z. 2018 Thymoquinone loaded in nanostructured lipid carrier showed enhanced anticancer activity in 4T1 tumor-bearing mice, *Nanomedicine.* 13 pp. 1567–1582. doi: 10.2217/nmm-2017-0322.
- Qu, S., Yang, H., Ren, D., Kan, S., Zou, G., Li, D., Li, M. 1999 Magnetite nanoparticles prepared by precipitation from partially reduced ferric chloride aqueous solutions, *J. Colloid Interface Sci.* 215 pp. 190–192. doi: 10.1006/jcis.1999.6185.
- Roca, A.G., Veintemillas-verdaguer, S., Port, M., Robic, C., Serna, C.J., Morales, M.P. 2009 Agents Based on High Quality Magnetite Nanoparticles, *J. Phys. Chem. B.* 113 pp. 7033–7039.
- Sambandam, S., Ramani, V. 2007 SPEEK/functionalized silica composite membranes for polymer electrolyte fuel cells, *J. Power Sources.* 170 pp. 259–267. doi: 10.1016/j.jpowsour.2007.04.026.
- Silva, V.A.J., Andrade, P.L., Silva, M.P.C., Bustamante, A.D., Valladares, L.D.L.S., Aguiar, J.A. 2013 Synthesis and characterization of Fe₃O₄ nanoparticles coated with fucan polysaccharides, *J. Magn. Magn. Mater.* 343 pp. 138–143. doi: 10.1016/j.jmmm.2013.04.062.
- Souza, K.C., Salazar-Alvarez, G., Ardisson, J.D., Macedo, W.A.A., Sousa, E.M.B. 2008 Mesoporous silica-magnetite nanocomposite synthesized by using a neutral surfactant, *Nanotechnology.* 19 pp. 1–3. doi: 10.1088/0957-4484/19/18/185603.
- Stober, E.B.W., Fink, A. 1968 Controlled Growth of Monodisperse Silica Spheres in the Micron Size Range, *J. Colloid Interface Sci.* 26 pp. 62–69.
- Teng, Y., Du, Y., Shi, J., Pong, P.W.T. 2020 Magnetic iron oxide nanoparticle-hollow mesoporous silica Spheres: Fabrication and potential application in drug delivery, *Curr. Appl. Phys.* 20 pp. 320–325. doi: 10.1016/j.cap.2019.11.012.
- Wu, W., He, Q., Jiang, C. 2008 Magnetic iron oxide nanoparticles: Synthesis and surface functionalization strategies, *Nanoscale Res. Lett.* 3 pp. 397–415. doi: 10.1007/s11671-008-9174-9.
- Wu, W., Wu, Z., Yu, T., Jiang, C., Kim, W.S. 2015 Recent progress on magnetic iron oxide nanoparticles: Synthesis, surface functional strategies and biomedical applications, *Sci. Technol. Adv. Mater.* 16 pp. 23501. doi: 10.1088/1468-6996/16/2/023501.
- Xie, Y., Kocaeefe, D., Chen, C., Kocaeefe, Y. 2016 Review of Research on Template Methods in Preparation of Nanomaterials, *J. Nanomater.* 2016. doi: 10.1155/2016/2302595.
- Zhang, H. 2020 Facile synthesis of hollow Fe₃O₄ nanospheres and their application as drug delivery carrier and anode for lithium-ion batteries, *Int. J. Electrochem. Sci.* 15 pp. 4789–4797. doi: 10.20964/2020.05.87.
- Zhang, L., Li, Y., Yu, J.C. 2014 Chemical modification of inorganic nanostructures for targeted and controlled drug delivery in cancer treatment, *J. Mater. Chem. B.* 2 pp. 452–470. doi: 10.1039/c3tb21196g.